# Mitochondrial division ensures the survival of postmitotic neurons by suppressing oxidative damage

Yusuke Kageyama,[1] Zhongyan Zhang,[1] Ricardo Roda,[1] Masahiro Fukaya,[2] Junko Wakabayashi,[1] Nobunao Wakabayashi,[3] Thomas W. Kensler,[3] P. Hemachandra Reddy,[4] Miho Iijima,[1] and Hiromi Sesaki[1]

[1]Department of Cell Biology, Johns Hopkins University School of Medicine, Baltimore, MD 21205
[2]Department of Anatomy, Kitasato University School of Medicine, Sagamihara, Kanagawa 252-0333, Japan
[3]Department of Pharmacology Chemical Biology, University of Pittsburgh School of Medicine, Pittsburgh, PA 15261
[4]Neurogenetics Laboratory, Neuroscience Division, Oregon National Primate Research Center, Oregon Health and Science University, Beaverton, OR 97006

Mitochondria divide and fuse continuously, and the balance between these two processes regulates mitochondrial shape. Alterations in mitochondrial dynamics are associated with neurodegenerative diseases. Here we investigate the physiological and cellular functions of mitochondrial division in postmitotic neurons using in vivo and in vitro gene knockout for the mitochondrial division protein Drp1. When mouse Drp1 was deleted in postmitotic Purkinje cells in the cerebellum, mitochondrial tubules elongated due to excess fusion, became large spheres due to oxidative damage, accumulated ubiquitin and mitophagy markers, and lost respiratory function, leading to neurodegeneration. Ubiquitination of mitochondria was independent of the E3 ubiquitin ligase parkin in Purkinje cells lacking Drp1. Treatment with antioxidants rescued mitochondrial swelling and cell death in Drp1KO Purkinje cells. Moreover, hydrogen peroxide converted elongated tubules into large spheres in Drp1KO fibroblasts. Our findings suggest that mitochondrial division serves as a quality control mechanism to suppress oxidative damage and thus promote neuronal survival.

## Introduction

Mitochondria form highly dynamic tubules, and are continuously fusing and dividing to control their size, number, and morphology. Loss of mitochondrial fusion generates many small mitochondria, while deficiency in the organelle's ability to divide leads to elongated mitochondria in most cells. The central components that mediate mitochondrial dynamics are three conserved dynamin-related GTPases (Okamoto and Shaw, 2005; Hoppins and Nunnari, 2009; Chang and Blackstone, 2010; Westermann, 2010; Kageyama et al., 2011; Tamura et al., 2011). In mammals, mitochondrial fusion is mediated by Mfns (mitofusin 1 and 2) and Opa1, which are located in the outer and inner membranes, respectively. Mitochondrial division is mediated by Drp1, which is mainly located in the cytosol. Drp1 is recruited to the mitochondrial surface by other outer membrane proteins (James et al., 2003; Yoon et al., 2003; Gandre-Babbe and van der Bliek, 2008; Otera et al., 2010; Palmer et al., 2011), where it assembles into spiral structures around mitochondria to induce fission of the mitochondrial membrane (Yoon et al., 2001; Lackner et al., 2009). The importance of mitochondrial dynamics to human health is highlighted by studies showing that mutations in Mfn2 and Opa1 underlie neurological disorders, including Charcot-Marie-Tooth disease type 2A and autosomal dominant optic atrophy, whereas a mutation in Drp1 causes neurodevelopmental abnormalities (Alexander et al., 2000; Delettre et al., 2000; Züchner et al., 2004; Waterham et al., 2007). Neurodegenerative disorders such as Alzheimer's disease, Parkinson's disease, and Huntington's disease are also associated with alterations in mitochondrial fusion and division (Cheung et al., 2007; Cho et al., 2010; Kageyama et al., 2011; Reddy et al., 2011).

Y. Kageyama and Z. Zhang contributed equally to this paper.

Correspondence to Hiromi Sesaki: hsesaki@jhmi.edu; or Miho Iijima: miijima@jhmi.edu

R. Roda's present address is National Institute of Neurological Disorders and Stroke, National Institutes of Health, Bethesda, MD 20892.

Abbreviations used in this paper: KO, knockout; MEF, mouse embryonic fibroblast, MEF; PDH, pyruvate dehydrogenase; ROS, reactive oxygen species.



The Rockefeller University Press $30.00
J. Cell Biol. Vol. 197 No. 4 535–551
www.jcb.org/cgi/doi/10.1083/jcb.201110034

Understanding the physiological and cellular functions of mitochondrial dynamics in mammals is one of the most fundamental questions in biology. As different cell types contain various amounts, shape, and distribution of mitochondria, it is crucial to decipher the in vivo roles of mitochondrial fusion and division in specific cell types. Mitochondrial fusion has been studied in several tissues using mouse models. Complete deletion of the genes encoding Mfns or Opa1 causes embryonic lethality (Chen et al., 2003; Zhang et al., 2011). Heterozygous loss of mouse Opa1 led to degeneration of the optic nerve, similar to human autosomal dominant optic atrophy (Alavi et al., 2007; Davies et al., 2007). Studies using tissue-specific deletion of Mfns and Opa1 have shown that mitochondrial fusion is important for the maintenance of functional mitochondrial DNA in neurons and skeletal muscle (Chen et al., 2007, 2010), as well as for the abundance of electron transport chain Complex IV, independent of mitochondrial DNA maintenance in pancreatic β cells (Zhang et al., 2011).

In contrast to mitochondrial fusion, research into the physiological role of mitochondrial division has only just begun. Recent studies have demonstrated that Drp1 is required for embryonic and brain development in mice (Ishihara et al., 2009; Wakabayashi et al., 2009). Drp1 knockout (KO) in the cerebellum during embryonic brain development altered mitochondrial morphology in Purkinje cells from short tubules to large spheres (Wakabayashi et al., 2009). However, mitochondria in granule cells appeared to be unaffected and remained tubular. In these mice, Drp1KO Purkinje cells were defective in cell proliferation. These data demonstrate that Purkinje cell development depends highly on Drp1 for mitochondrial division, and that these cells represent a good neuronal model for studying this process. Given the links between neurodegenerative diseases and mitochondrial division, it is important to understand the role of Drp1 in postmitotic neurons after completion of development. Because the mice used in previous studies lose Drp1 during development and die during or immediately after birth, the role of mitochondrial division in the survival of postmitotic neurons remains unanswered. Here, we analyzed the function of Drp1 in postmitotic Purkinje cells using mouse models and primary cell culture and found that loss of Drp1 led to an accumulation of oxidative damage, decreased respiratory function, and neurodegeneration. Moreover, Purkinje cell death was rescued by treatment with antioxidants. Our study shows that mitochondrial division suppresses oxidative damage and therefore protects neurons from degeneration.

## Results

### Loss of Drp1 causes Purkinje cell degeneration

We deleted Drp1 in postmitotic Purkinje cells using L7-Cre, which establishes the expression of Cre recombinase at around 3 wk after birth in these cells (Barski et al., 2000). Purkinje cells largely differentiate postnatally and undergo morphological changes in 3 wk after birth, including the extension of axons and dendrites (Hatten et al., 1997; Chizhikov and Millen, 2003). Through breeding, we generated *Drp1*$^{flox/flox}$*::L7-Cre* mice (L7-Drp1KO) and littermate controls. L7-Drp1KO and control mice were viable, fertile, and normal in size. Cerebellum of mice ranging in age from 1–6 mo was fixed, dissected, and sectioned around the median line. To examine the effect of Drp1 knockout on Purkinje cells, cerebellar sections were subjected to immunofluorescence with antibodies against the Purkinje cell marker carbonic anhydrase 8 (Car8; Wakabayashi et al., 2009), and soma were counted to quantify the number of Purkinje cells (Fig. 1, A and B). At 1 mo, the pattern and number of Purkinje cells were indistinguishable between control and L7-Drp1KO mice. Large dendritic arbors were observed in both control and L7-Drp1KO Purkinje cells. At 2 mo, although the number of Purkinje cells was not significantly decreased, we noticed the onset of Purkinje cell degeneration in L7-Drp1KO mice. Co-immunostaining with anti-Drp1 antibodies confirmed that 70 and 85% of Purkinje cells lost Drp1 expression in L7-Drp1KO mice at 1 and 2 mo, respectively (Fig. S1, A and B). Strikingly, at 3 mo, ∼40% of Purkinje neurons had degenerated in L7-Drp1KO mice. At 6 mo, 90% of Purkinje cells were lost in L7-Drp1KO mice. Conversely, Purkinje cells were normal in control mice at all ages examined. We verified these results using another Purkinje cell maker, calbindin. TUNEL assay and immunohistochemistry using antibodies to activated caspase-3 provided no evidence for apoptosis in the cerebellum of L7-Drp1KO mice (unpublished data). Hematoxylin and eosin staining also showed loss of Purkinje cells in the knockout animals (Fig. 1 C). The soma of Purkinje cells was easily observed in the Purkinje cell layer in control mice. In contrast, at 6 mo L7-Drp1KO mice lacked the Purkinje cell layer. Moreover, rotarod tests revealed that motor coordination in L7-Drp1KO mice was compromised (Fig. 1 D). Although control and L7-Drp1KO mice showed indistinguishable behaviors at 1–3 mo, 4–6-mo-old Drp1 conditional knockout mice exhibited increasing motor deficiencies and fell off the rod more quickly than control mice.

### Swollen mitochondria in L7-Drp1KO Purkinje cells

To examine mitochondrial morphology in Purkinje cells, cerebellar sections were stained using antibodies to pyruvate dehydrogenase (PDH), a matrix protein, and Car8. In contrast to the short tubular structures seen in control mice, mitochondria in Purkinje cells were large spheres in L7-Drp1KO mice as early as 1 mo of age (Fig. 2 A). Swelling of mitochondria appeared to occur in the soma and distal portions of dendrites at 1–2 mo, and then mitochondria in proximal portions of dendrites became enlarged at later ages (Fig. 2 B). Electron microscopy confirmed the large round morphology of mitochondria in Purkinje cells of L7-Drp1KO mice (Fig. 2 C). Mitochondria displayed a wild-type morphology in Purkinje cells of 2-wk-old L7-Drp1KO mice (unpublished data). Quantification of mitochondrial morphology showed that 25 and 60% of Purkinje cells contain large spherical mitochondria at 1 and 2 mo of age, respectively, in L7-Drp1KO mice (Fig. 2 D). As the majority of Purkinje cells are maintained at 2 mo in L7-Drp1KO mice (Fig. 1 B), mitochondria likely enlarge before the degeneration of Purkinje cells. In addition, given that Drp1 expression was already lost in

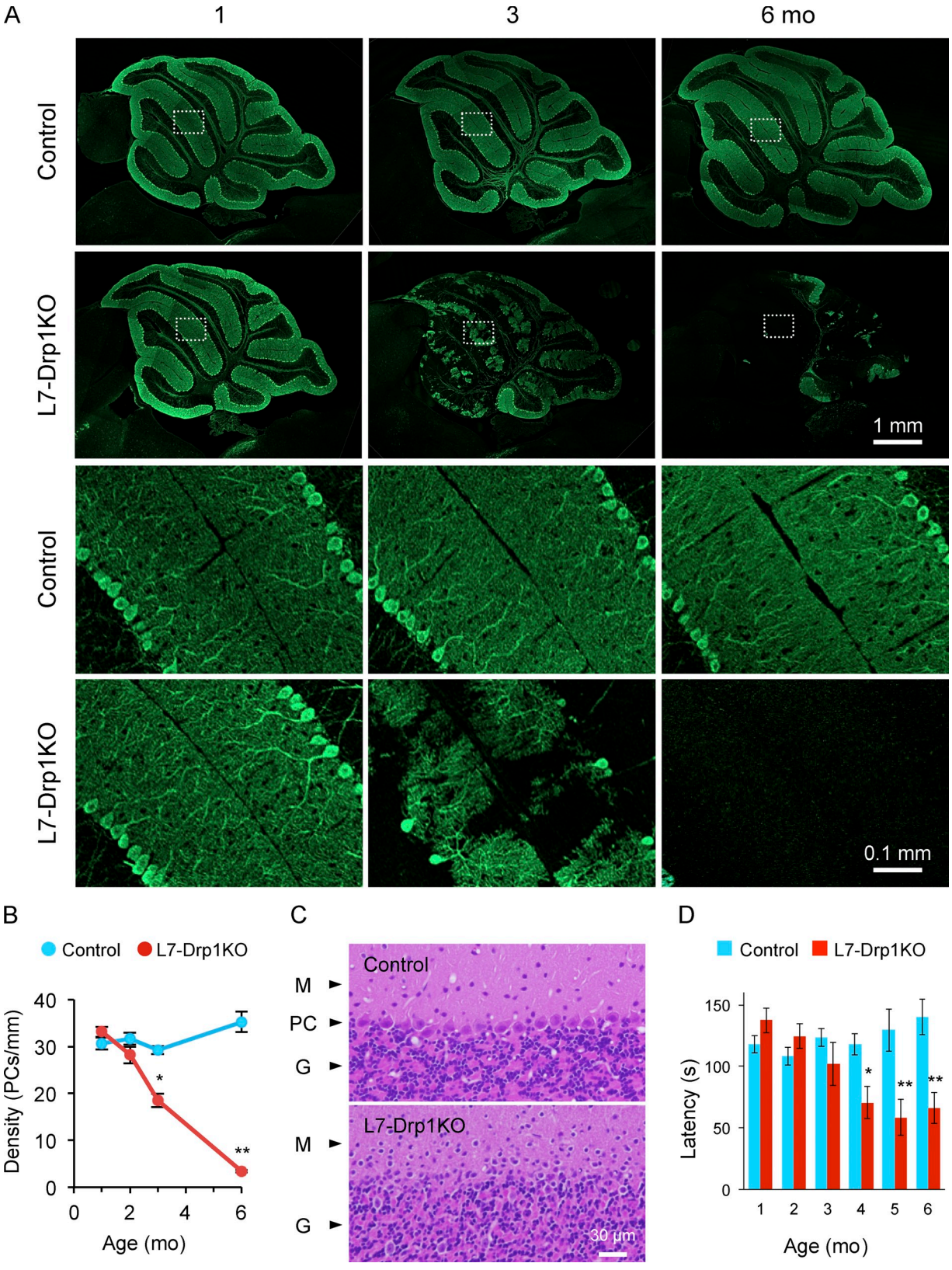


Figure 1. **Purkinje cells degenerate in L7-Drp1KO mice.** (A) Immunofluorescence of cerebellar sagittal sections around the median line using antibodies to Car8, a Purkinje neuron marker. Control and L7-Drp1KO mice were analyzed at the indicated ages. Boxed regions show magnified images. (B) Quantification of Purkinje cell density. The number of soma of Purkinje cells was determined and normalized relative to the length of the Purkinje cell layer. Values represent the mean ± SEM ($n \geq 3$). (C) Hematoxylin and eosin stains of cerebellar sagittal sections at 6 mo. The Purkinje cell layer (PC) was lost in L7-Drp1KO mice. M, molecular layer; G, granule cell layer. (D) Rotarod tests. To examine motor coordination ability, the latency to fall from the rotarod was determined in control and L7-Drp1KO mice. Values represent the mean ± SEM ($n \geq 5$).

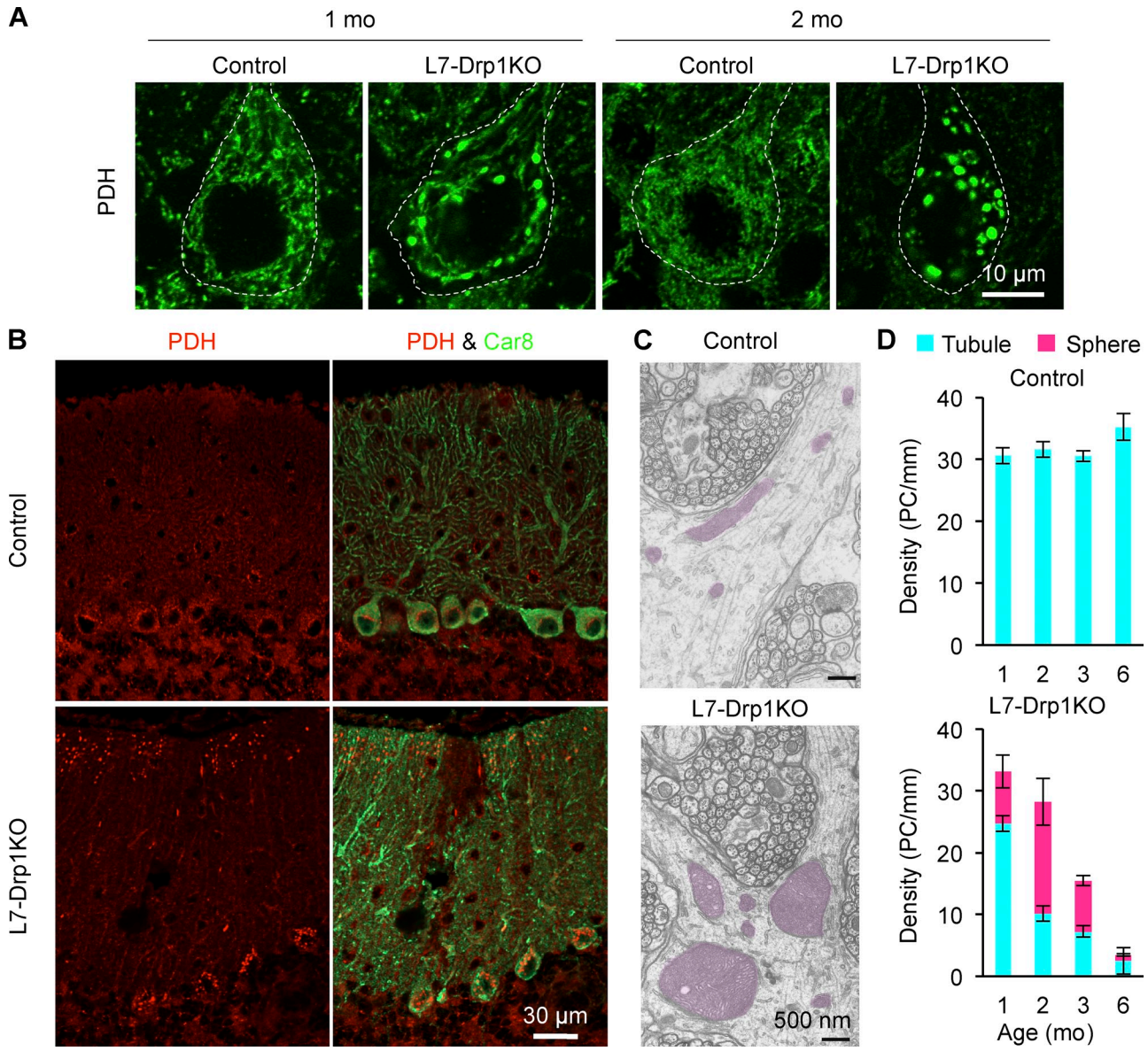


Figure 2. **Mitochondria are swollen in Drp1KO Purkinje cells.** (A) Mitochondrial morphology. Sagittal sections of the cerebellum in control and L7-Drp1KO mice at the indicated ages were stained using antibodies against Car8 and PDH. The soma of Purkinje cells are outlined based on Ca8 staining (dotted line). (B) Distribution of enlarged mitochondria. Lower magnification images of cerebellar sections stained with antibodies to PDH and Car8. Swollen mitochondria were observed in the soma and distal portions of dendrites in L7-Drp1KO Purkinje cells at 2 mo. Mitochondria appeared to be tubular in other regions of L7-Drp1KO Purkinje cells. (C) Electron microscopy of mitochondria in dendrites in control and L7-Drp1KO Purkinje cells. Mitochondria are highlighted in red. (D) Quantification of mitochondrial morphology. The number of soma of Purkinje cells that contain tubular or large spherical mitochondria was determined and normalized relative to the length of the Purkinje cell layer. Values represent the mean ± SEM ($n \geq 4$).

~70% of Purkinje cells in L7-Drp1KO mice at 1 mo (Fig. S1, A and B), we estimate that swelling of mitochondria takes a couple of weeks after Drp1 loss.

We examined the morphology of peroxisomes by immunofluorescence using anti-Pex14 antibodies as Drp1 also participates in peroxisomal division (Schrader, 2006). Peroxisomes in control and L7-Drp1KO Purkinje cells were indistinguishable and displayed small round structures (Fig. S1 C). This phenotype is different from Drp1KO MEFs, in which peroxisomes are elongated (Wakabayashi et al., 2009). Peroxisomal division may be less dependent on Drp1 in Purkinje cells. Our data indicate that the degeneration of Purkinje cells likely results from defects in mitochondria division in L7-Drp1KO mice.

### Impaired electron transport chain activities in L7-Drp1KO Purkinje cells

To determine whether Drp1 loss affects mitochondrial respiratory functions in Purkinje cells, we analyzed the activity of electron transport chain complexes in histochemical assays using frozen sections of L7-Drp1KO cerebellum (Fig. 3 A; De Paepe et al., 2009). NADH dehydrogenase (NDH, Complex I) and cytochrome *c* oxidase (COX, Complex IV) showed similar activity in the Purkinje cell layer of 1-mo-old control and L7-Drp1KO mice (Fig. 3 A). However, at 2 mo, their activities were dramatically decreased in the Purkinje cell layer of L7-Drp1KO mice. At this age, most Purkinje cells were maintained in L7-Drp1KO mice (Figs. 1 B and 3 A, Car8), suggesting that

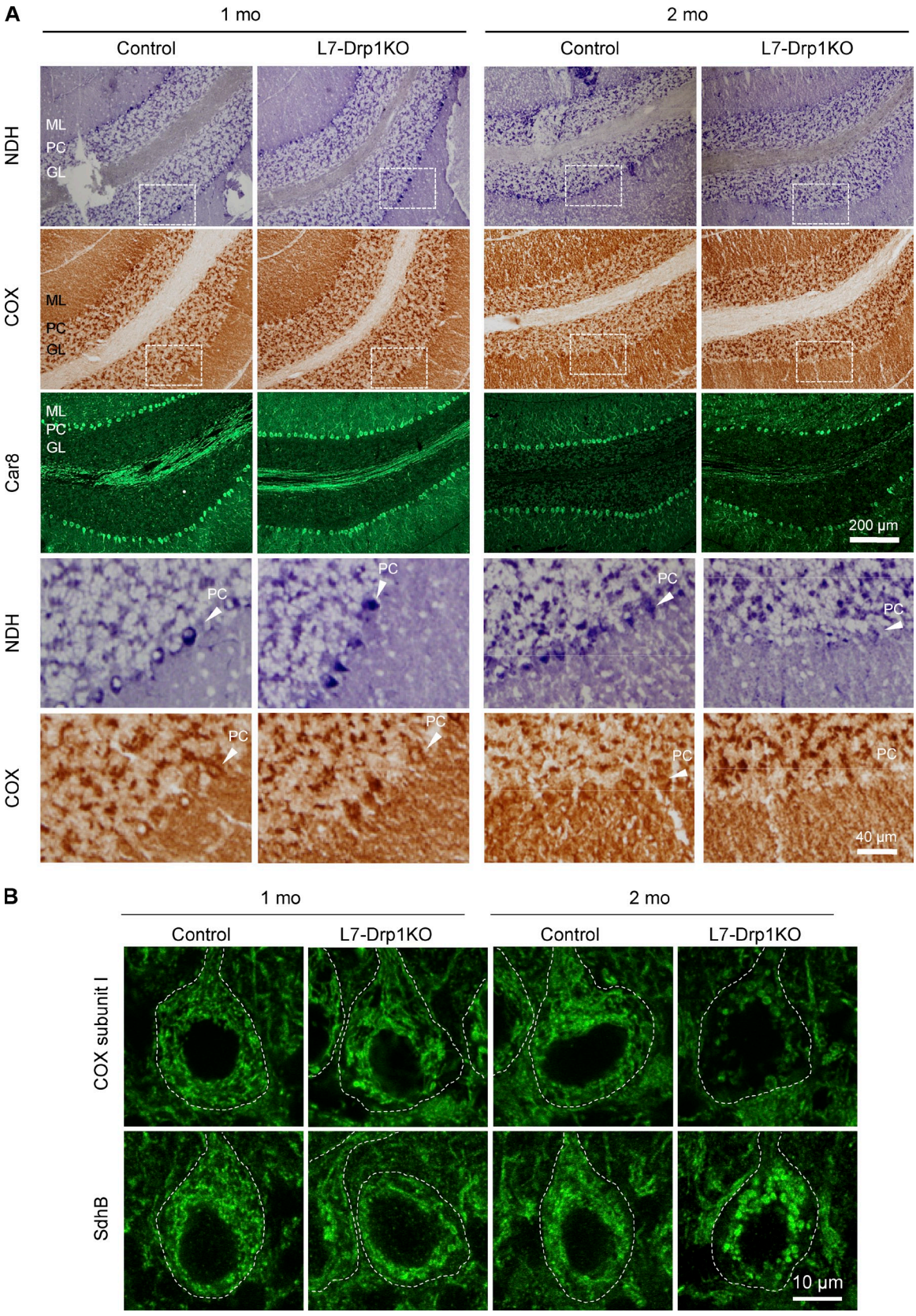


Figure 3. **Decreased respiratory activities in L7-Drp1KO Purkinje cells.** (A) Fresh frozen cerebellar sections of control and L7-Drp1KO mice at the indicated ages were stained for NADH dehydrogenase activity, COX activity, and Car8. Sagittal sections of the cerebellum around the median line were used. Boxed regions show magnified images. PC, Purkinje cell layer; M, molecular layer; G, granule cell layer. (B) Sagittal sections of the cerebellum in control and L7-Drp1KO mice at the indicated ages were stained using antibodies against Car8, cytochrome *c* oxidase subunit I (COX subunit I), or succinate dehydrogenase iron-sulfur subunit (SdhB). The soma of Purkinje cells are outlined based on Ca8 staining (dotted line).

decreases in electron transport chain activities precede Purkinje cell death.

Consistent with the reduced activities of electron transport chain complexes in L7-Drp1KO mice, we found decreased levels of COX subunit I in L7-Drp1KO Purkinje cells at 2 mo, but not 1 mo (Fig. 3 B and Fig. S2). Levels of COX subunit I were unaffected in granule cells from the same sections (Fig. S2, red box). Decreased levels of subunit I may at least partially contribute to the reduction in COX activity. The amounts of both PDH and succinate dehydrogenase iron-sulfur subunit did not decrease in either 1- or 2-mo-old L7-Drp1KO mice (Figs. 2 A and 3 B). Therefore, the reduced levels of COX subunit I observed were not simply due to a general reduction in mitochondrial proteins.

Previous studies have shown that functionally compromised mitochondria are subjected to turnover by autophagy, which requires ubiquitination of mitochondrial proteins and proteasomal degradation (Narendra et al., 2008; Twig et al., 2008; Tanaka et al., 2010; Yoshii et al., 2011). When we examined cerebellar sections using immunofluorescence with antibodies to ubiquitin and the mitochondrial outer membrane protein Tom20, we observed increases in ubiquitin staining associated with large spherical mitochondria in L7-Drp1KO Purkinje cells over time (Fig. 4 A). Quantification showed that 40 and 50% of Purkinje cells contain mitochondria that are positive for ubiquitin staining at 1 and 2 mo of age, respectively, in L7-Drp1KO mice (Fig. 4 B). We did not observe ubiquitin accumulation in control Purkinje cells, however. Thus, it is likely that mitochondria were not efficiently degraded in the L7-Drp1KO Purkinje cells, causing ubiquitinated proteins to accumulate with age.

Studies have shown that an E3 ubiquitin ligase called parkin ubiquitinates mitochondrial proteins to promote proteasomal degradation and mitophagy (Narendra et al., 2008; Tanaka et al., 2010). To determine whether parkin is required for ubiquitination in L7-Drp1KO Purkinje cells, we generated *Parkin*$^{-/-}$ (ParkinKO)::L7-Drp1KO mice by breeding. Our results demonstrate that loss of parkin did not decrease mitochondrial ubiquitination and swelling in Purkinje cells in ParkinKO::L7-Drp1KO mice (Fig. 4 C). These data indicate that mitochondrial ubiquitination due to Drp1 deficiency occurs independently of parkin in vivo.

### Treatment with hydrogen peroxide swells mitochondria in Drp1KO MEFs

We sought to understand how mitochondria become swollen in L7-Drp1KO Purkinje cells but not in Drp1KO MEFs. Because neurons consume large amounts of oxygen and are vulnerable to reactive oxygen species (ROS; Cui et al., 2004), we tested whether oxidative stress can transform elongated tubules into large balls in Drp1KO MEFs. When Drp1KO MEFs were treated with hydrogen peroxide (50 µM), the morphology of mitochondria in Drp1KO MEFs changed from elongated tubules to enlarged spheres in a time-dependent manner (Fig. 5). This effect was inhibited by co-incubation with the antioxidant *N*-acetylcysteine (1 mM; Fig. S3). During hydrogen peroxide treatment, mitochondria appeared to be partially severed in both wild-type and Drp1KO MEFs. We have shown previously that Drp1KO MEFs undergo a low level of mitochondrial division activity (Wakabayashi et al., 2009), which may mediate the partial fragmentation of mitochondria in Drp1KO MEFs. Treatments with carbonylcyanide-3-chlorophenylhydrazone, which dissipates the membrane potential across the inner membrane, or nocodazole, which disrupts microtubules, did not induce mitochondrial enlargement (Fig. S3), suggesting that mitochondrial swelling is not a secondary consequence of reduced membrane potential or dissociation from the cytoskeleton, consistent with previous reports (Smirnova et al., 2001; Gandre-Babbe and van der Bliek, 2008; Palmer et al., 2011).

### Mitochondrial division is required for the distribution of mitochondria in dendrites during neurite extension

To gain further insight into the roles of mitochondrial division in cell survival and mitochondrial morphology in Purkinje cells, cerebellar neurons were isolated from P0 *Drp1*$^{flox/flox}$ mice and cultured in vitro. Immediately after isolation, Purkinje cells appeared to be round, and subsequently underwent morphological differentiation to extend axons and dendrites in ∼10 d of culture (Fig. 6, A and C). We infected neurons with lentiviruses expressing the Cre recombinase to delete Drp1 at two different time points. In the first set of experiments, lentiviruses were added to the cerebellar neuron culture when the cells were plated (termed "day 0 infection") to study mitochondrial division during differentiation. In the other set of experiments, we infected cerebellar neurons at d 7 (termed "day 7 infection") to study mitochondrial division in Purkinje cells that already have extended dendrites and axons. As described below, these experiments revealed different yet overlapping requirements for mitochondrial division in Purkinje cells.

For day 0 infection, we used lentiviruses carrying the Cre recombinase and GFP in tandem to delete Drp1 (Drp1KO culture). This virus allowed us to monitor infection efficiency and we used a condition in which virtually all cells expressed GFP. As a control, GFP-carrying lentiviruses were used (control culture). Cultured neurons were stained using antibodies to the Purkinje cell marker calbindin at d 10 and 20 (Fig. 6, A and B). After 10 d in culture, the number of Purkinje cells started to decrease in the Drp1KO cultures. After 20 d in culture, the number of Purkinje cells in the Drp1KO culture was decreased significantly. Assessment of total cell number using DAPI staining revealed no differences at both d 10 and 20 between the two cultures, in which granule cells are predominant (Furuya et al., 1998; Tabata et al., 2000). These results suggest that the cell death was specific to Purkinje cells. Because these cells represent only a small fraction of all the cells in this culture (<1%), the loss of Purkinje cells did not affect the total cell number significantly.

To observe mitochondria in Purkinje cells, we used lentiviruses carrying only the Cre recombinase to delete Drp1, which enabled us to stain Car8 to identify Purkinje cells, PDH for the mitochondrial matrix, and Tom20 for the mitochondrial outer membrane. Lentiviruses carrying the myc epitope were used as a control. In control Purkinje cells, mitochondria displayed short tubular structures and were distributed evenly throughout

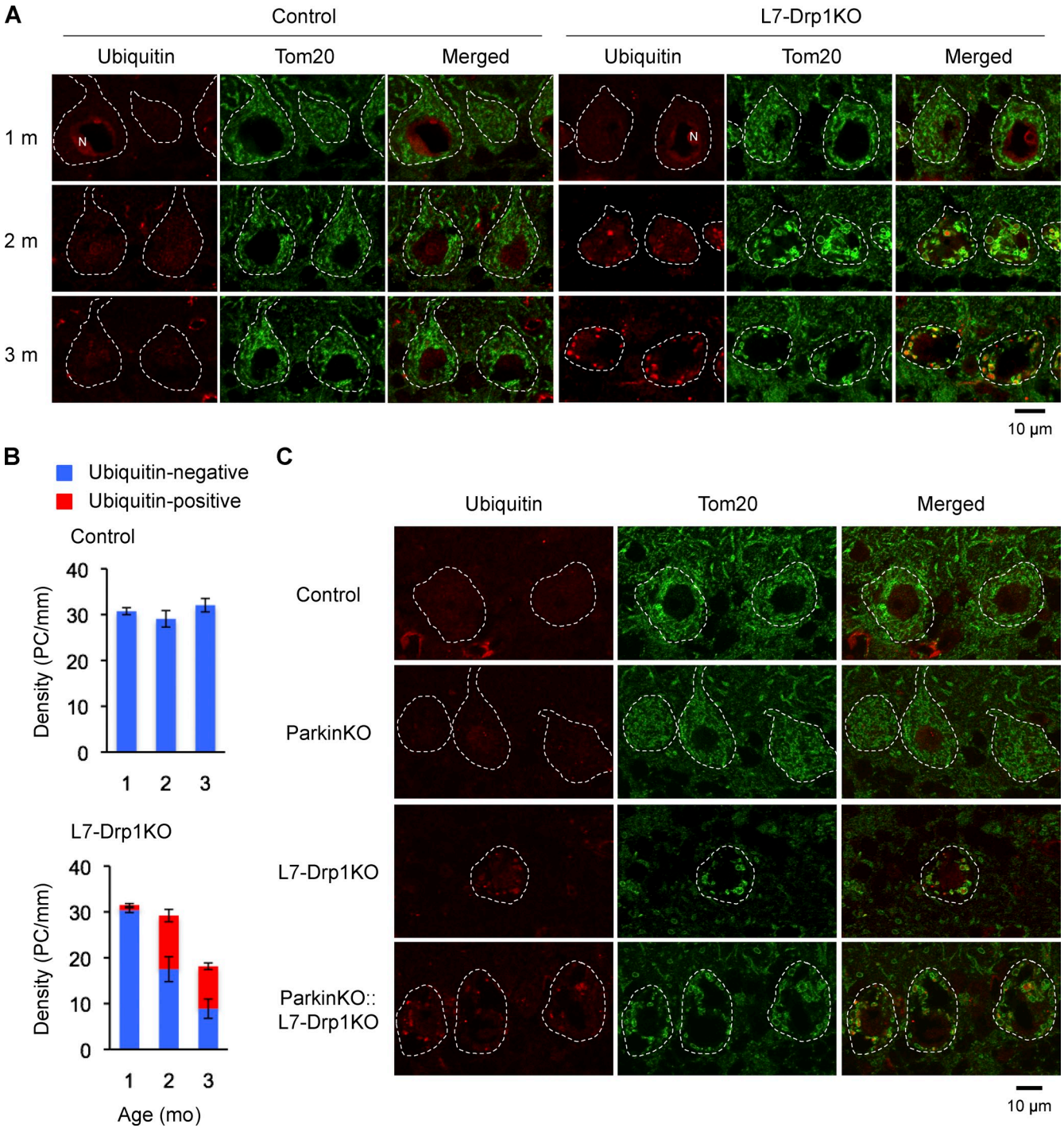


Figure 4. **Ubiquitination of mitochondria in L7-Drp1KO Purkinje cells.** (A) Sections of the cerebellum in control and L7-Drp1KO mice at 1–3 mo were stained using antibodies to ubiquitin, Tom20, and Car8. Nuclei (N) were stained by anti-ubiquitin antibody due to ubiquitination of histones as reported previously (Muratani and Tansey, 2003). (B) Quantification of ubiquitin staining. The number of soma of Purkinje cells (PC) that contain mitochondria positive (red) and negative (blue) for ubiquitin staining was determined and normalized relative to the length of the Purkinje cell layer. Values represent the mean ± SEM ($n \geq 3$). (C) Sections of the cerebellum in control, ParkinKO, L7-Drp1KO, and ParkinKO::L7-Drp1KO mice at 2 mo were stained using antibodies to ubiquitin, Tom20, and Car8. The soma of Purkinje cells are outlined based on Car8 staining (dotted line).

the soma, dendrites, and axons (Fig. 6 C). In Drp1KO Purkinje cells, PDH staining showed that mitochondria were swollen as observed in vivo. Interestingly, Tom20 staining revealed elongated outer membranes that appeared to connect spherical portions of mitochondria. In addition to morphological changes, Drp1KO Purkinje cells contained fewer mitochondria in their dendrites. Most mitochondria were distributed in the soma and axons, which were morphologically identified as the longest extension without spines. Inside axons, several mitochondrial tubules appeared to run in parallel based on Tom20 staining. These results indicate that mitochondrial division is required for the distribution of mitochondria in dendrites.

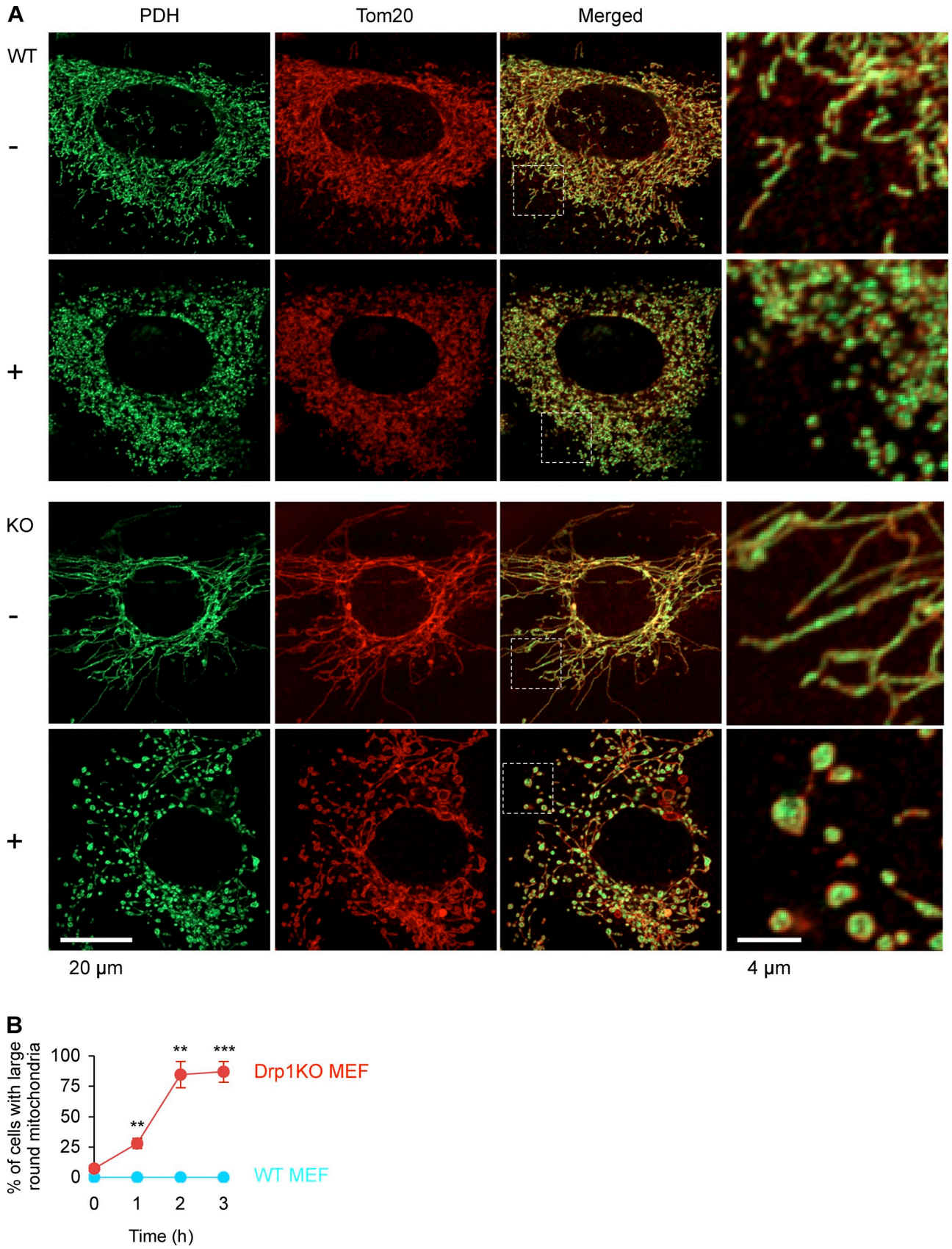


Figure 5. **Hydrogen peroxide treatment enlarges mitochondria in Drp1KO MEFs.** (A) Wild-type and Drp1KO MEFs were incubated in the presence and absence of 50 µM hydrogen peroxide for 1, 2, and 3 h. Cells were then fixed and subjected to immunofluorescence with antibodies to PDH and Tom20. Images at 2 h are shown. (B) Time course of mitochondrial enlargement. Cells that contained enlarged mitochondria were scored. Values represent the mean ± SEM ($n$ = 3). More than 100 cells were examined in each experiment.

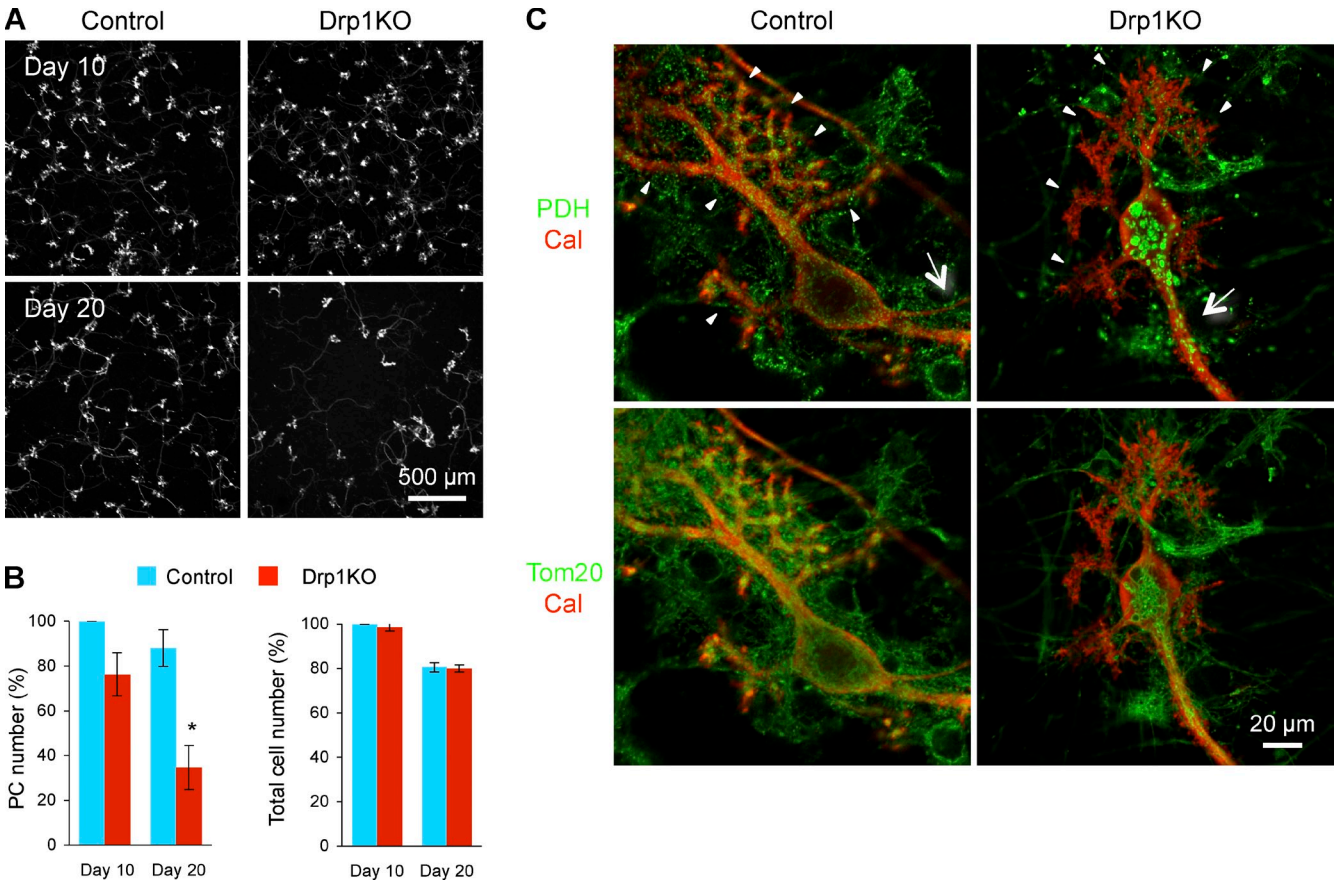


Figure 6. **Purkinje cells die after Drp1 loss in vitro.** (A) Cerebellar neurons were isolated from P0 *Drp1*$^{flox/flox}$ mice and cultured for 20 d. When cells were plated (d 0), lentiviruses carrying Cre recombinase and GFP in tandem (Drp1KO) or GFP alone (control) were added to the culture. At d 10 and 20, cells were fixed and analyzed by immunofluorescence using anti-calbindin antibodies. (B) Quantification of the number of Purkinje cells and total cells. To count the number of Purkinje cells and total cells, calbindin staining and DAPI staining were used, respectively. Cell numbers were normalized to those of control cells at d 10 in each experiment. Values represent the mean ± SEM ($n$ = 3). (C) Cultured cerebellar neurons were infected with lentiviruses carrying the Cre recombinase (Drp1KO) and the myc epitope (control). Mitochondria were visualized with immunofluorescence using antibodies to PDH, calbindin, and Tom20 in control and Drp1KO Purkinje cells at d 10. Dendrites and axons are indicated by arrowheads and arrows, respectively.

To further explore mechanisms underlying the lack of mitochondria in dendrites, we examined mitochondrial distribution at different time points during neurite extension (Fig. S4). Axons were found to grow before mitochondrial swelling and therefore small mitochondria were already transported to axons (Fig. S4, day 3). Dendrites extended after mitochondria became large spheres (Fig. S4, day 6 and day 8). At these time points, mitochondria in axons also became swollen (Fig. S4, day 6 and day 8). These results suggest that increases in the size of mitochondria block efficient transport of mitochondria into dendrites in Drp1 KO Purkinje cells.

As we observed in vivo, large spherical mitochondria were stained by anti-ubiquitin antibodies in cultured Drp1KO Purkinje cells (Fig. 7, B and F). We also found increased oxidative damage associated with the swollen mitochondria in these cells using immunofluorescent staining with antibodies to an oxidative marker for both proteins and lipids, 4-hydroxynonenal (HNE), which is produced by lipid oxidation and modifies proteins (Fig. 7, C and F). Control Purkinje cells did not show HNE signals associated with mitochondria.

Mitophagy has been proposed to play important roles in turnover of damaged mitochondria (Youle and Narendra, 2011). To examine mitophagy in Drp1KO Purkinje cells, we performed immunofluorescence microscopy using an antibody to LC3, an autophagosome marker. We found that LC3 colocalizes with mitochondria in Drp1KO Purkinje cells, but not in control Purkinje cells (Fig. 7, D and F). In addition, p62/SQSTM1, an autophagosome protein that binds to both ubiquitin and LC3, was recruited to the mitochondria (Fig. 7, E and F). Interestingly, p62/SQSTM1 was associated with only a small fraction of mitochondria in Drp1KO Purkinje cells. Furthermore, LC3 was associated with swollen mitochondria in Purkinje cells in L7-Drp1KO mice (Fig. 8). Altogether, these results suggest that mitophagy is promoted and/or blocked in Drp1-null Purkinje cells.

### Drp1 deletion after d 7 of culture swells mitochondria and induces Purkinje cell death without affecting mitochondrial distribution

In the next set of experiments, we infected cultured cerebellar neurons with lentiviruses carrying the Cre recombinase (Drp1KO culture) or myc (control culture) at d 7 to delete Drp1 after Purkinje cells had extended their dendrites and axons. Cells were

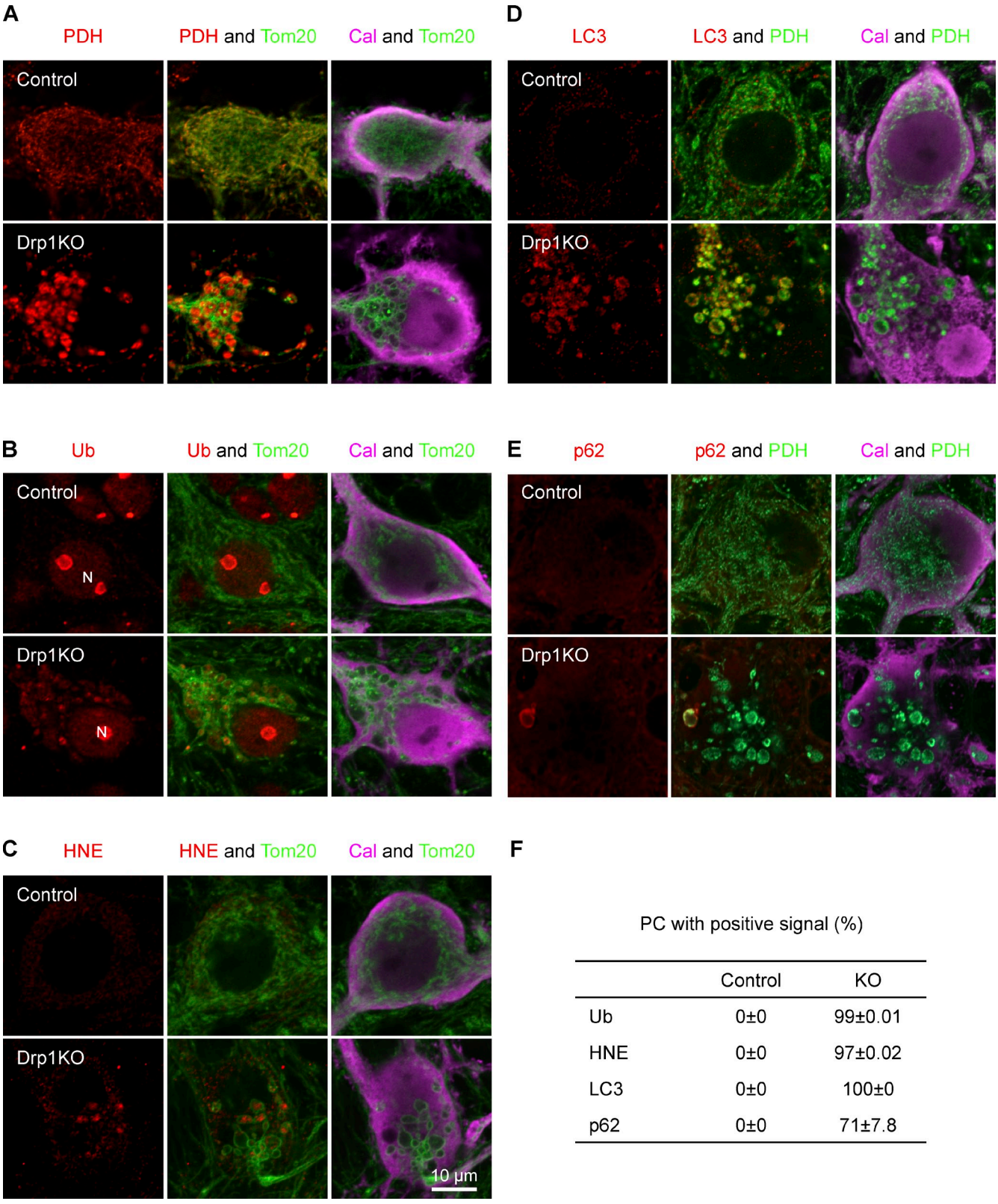


F

PC with positive signal (%)

| | Control | KO |
|---|---|---|
| Ub | 0±0 | 99±0.01 |
| HNE | 0±0 | 97±0.02 |
| LC3 | 0±0 | 100±0 |
| p62 | 0±0 | 71±7.8 |

Figure 7. **Mitochondria accumulate autophagy markers in cultured Drp1KO Purkinje cells.** (A–E) Cultured cerebellar neurons were infected with lentiviruses carrying the Cre recombinase (Drp1KO) and the myc epitope (control) at d 0 and cultured for 20 d. Immunofluorescence was performed using antibodies to calbindin to identify Purkinje cells, PDH, and Tom20 to label mitochondria, as well as antibodies to ubiquitin (B), 4-hydroxynonenal (HNE) (C), LC3 (D), and p62/SQSTM1 (E). The soma of Purkinje cells are shown. Nuclei (N) were stained due to ubiquitination of histones (Muratani and Tansey, 2003) in B. (F) Quantification of the number of Purkinje cells containing mitochondria with positive staining for the indicated marker. Values represent the mean ± SE.

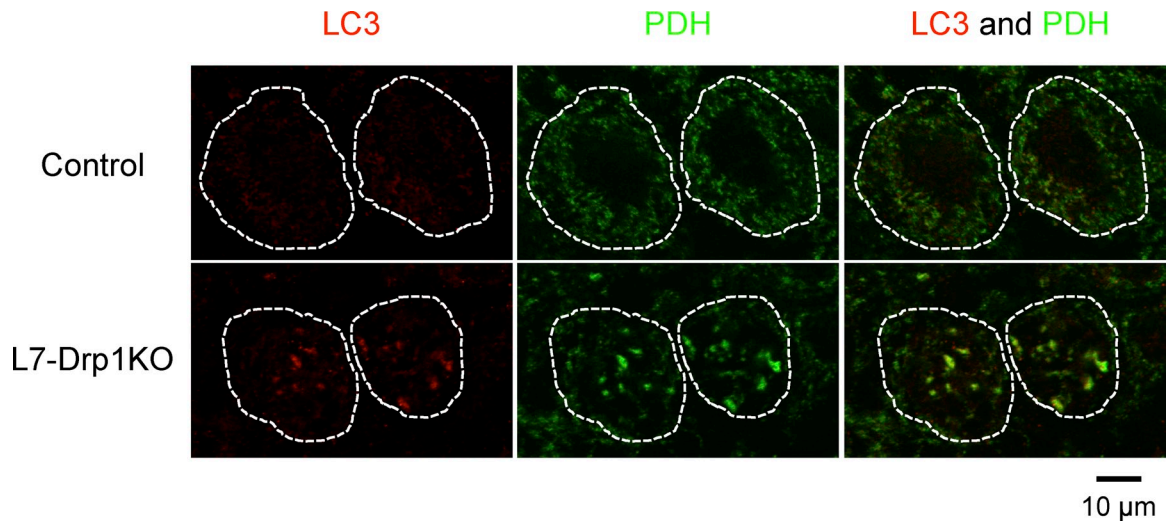


Figure 8. **Mitochondria accumulate LC3 in Purkinje cells in L7-Drp1KO mice.** Sections of the cerebellum in control and L7-Drp1KO mice at 2 mo were stained using antibodies to LC3. Antibodies to Car8 and PDH were used to label Purkinje cells and mitochondria, respectively. The soma of Purkinje cells are outlined based on Car8 staining (dotted line).

subjected to immunofluorescence using antibodies to PDH and calbindin at d 20 and 30 (e.g., 13 and 23 d after infection). Similar to day 0 infection, we found increased Purkinje cell death in the Drp1KO culture (Fig. 9 A, left graph). At d 20, the number of Purkinje cells in the Drp1KO culture was slightly decreased. At d 30, the number was ∼50% that of the control culture. Indistinguishable numbers of DAPI-stained cells were observed in the control and Drp1KO cultures, suggesting that, like day 0 infection, cell death was specific to Purkinje cells (Fig. 9 A, middle graph). At both d 20 and 30, ∼45% of Purkinje cells in the Drp1KO culture contained swollen mitochondria (Fig. 9 A, right graph; Fig. 9 B). The mitochondria appeared normal in the remaining Purkinje cells, which is presumably due to lower infection efficiency. In the control culture, all Purkinje cells contained short tubular mitochondria. Like day 0 infection, increased HNE staining was associated with large spherical mitochondria in the Drp1KO Purkinje cells (Fig. 9 C). Unlike day 0 infection, swollen mitochondria were found in dendrites in addition to the soma and axons in Drp1KO Purkinje cells in the day 7 infection culture (Fig. 9, B and C). Thus, mitochondrial division is critical for the distribution of mitochondria in Purkinje cells during dendritic extension, but is dispensable for the maintenance of mitochondrial distribution in Purkinje cells with previously extended dendrites.

### Treatment with antioxidants suppresses mitochondrial swelling and cell death in Drp1KO Purkinje cells in vitro and in vivo

Our data suggest that mitochondria in neurons become swollen due to ROS. Similarly, the death of Purkinje cells may result from oxidative damage. To address these questions, we add the antioxidant *N*-acetylcysteine to d 7 infected Purkinje cell culture concomitantly to infection. Treatment with 1 mM *N*-acetylcysteine led to a fourfold suppression of mitochondrial enlargement in Drp1KO Purkinje cells (Fig. 9 A, right graph; Fig. 9 B). *N*-acetylcysteine–treated Drp1KO Purkinje cells contained elongated mitochondria similar to Drp1KO MEFs. Similarly, a mitochondria-targeted antioxidant, MitoQ (Manczak et al., 2010), suppressed mitochondrial swelling (Fig. S5), suggesting that ROS from both mitochondria and the cytosol contribute to changing mitochondrial shape.

*N*-acetylcysteine also rescued cell death in Drp1KO Purkinje cells, as similar numbers of Purkinje cells were observed in the control and Drp1KO cultures on both d 20 and 30 (Fig. 9 A, left graph). Next, we further tested whether antioxidants improve Purkinje cell survival in the absence of Drp1 at the animal level. We fed L7-Drp1KO mice with control and coenzyme Q10–containing diets from 3 wk of age and examined neurodegeneration and mitochondrial morphology at 3 mo. Results show that coenzyme Q10 significantly increased the number of Drp1KO Purkinje cells that contain tubular mitochondria and suppressed neurodegeneration (Fig. 10 A). Thus, decreasing ROS levels prevents mitochondrial swelling and cell death in Drp1KO Purkinje cells.

## Discussion

Our study demonstrates the physiological and cellular functions of mitochondrial division in the survival of mammalian neurons. We show that the loss of Drp1 in postmitotic Purkinje cells leads to degeneration in mouse models and primary cell culture. In the absence of mitochondrial division, this organelle accumulates oxidative damage, exhibits decreased respiratory functions, and become ubiquitinated. The rescue of Purkinje cell death by antioxidant treatment supports the model that mitochondrial division protects neurons from oxidative damage. Our data also provide evidence that mitochondrial division is critical for mitochondrial quality control in a physiological context.

It has been shown that deficiency in mitochondrial division leads to two major morphological consequences. Without the ability to divide, mitochondria elongated and interconnected

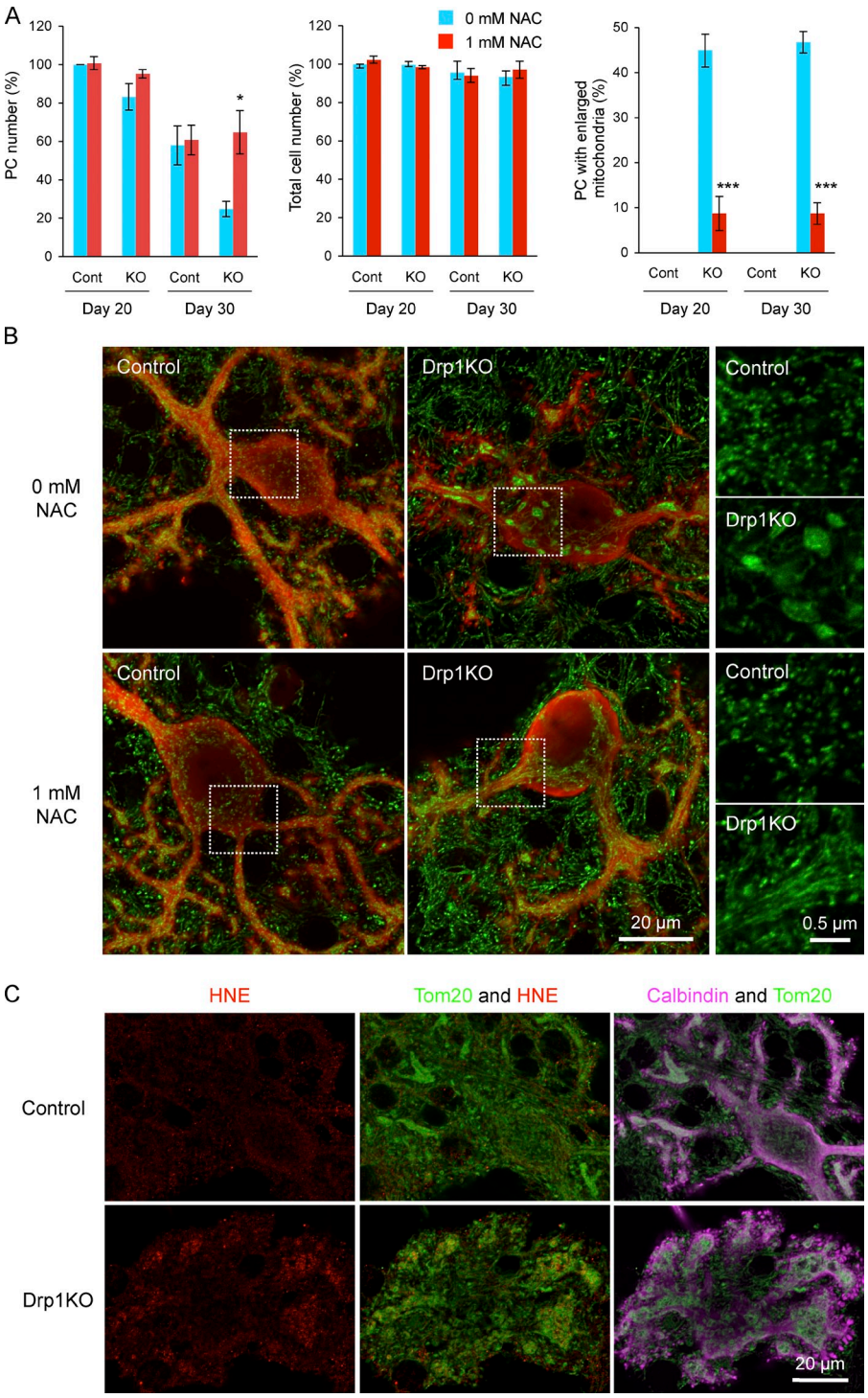


Figure 9. ***N*-acetylcysteine suppresses mitochondrial enlargement, cell death, and oxidative damage in Drp1KO Purkinje cells.** (A) Cerebellar neurons were isolated from P0 *Drp1*$^{flox/flox}$ mice and cultured for 30 d. At d 7, lentiviruses carrying the Cre recombinase (Drp1KO) or the myc epitope (control) were added to the culture medium. At the same time, cells were left untreated or treated with 1 mM *N*-acetylcysteine. At d 20 and 30, cells were fixed and analyzed by immunofluorescence using anti-calbindin antibodies. The number of Purkinje cells was quantified (left graph). DAPI staining was used to determine the total cell number (middle graph), which was normalized to that of untreated control cells at d 20 in each experiment. Purkinje cells that contained enlarged mitochondria were quantified (right graph). Values represent the mean ± SEM ($n$ = 4). (B) Immunofluorescence of control and Drp1KO Purkinje cells was performed with antibodies against PDH (green) and calbindin (red) at d 20. Boxed regions show magnified images of mitochondria. (C) Immunofluorescence of control and Drp1KO Purkinje cells using antibodies to 4-hydroxynonenal (HNE), Tom20, and calbindin at d 30.

in most cells lines and MEFs or became large spheres in several neurons including Purkinje cells (Ishihara et al., 2009; Wakabayashi et al., 2009). However, what determines such mitochondrial morphologies was unknown. We found that antioxidant treatment can suppress mitochondrial swelling in Drp1KO Purkinje cells, whereas increased ROS levels can convert elongated tubules into large round structures in Drp1KO MEFs. These data indicate that loss of mitochondrial division first causes elongation of mitochondria due to excess fusion and subsequent accumulation of oxidative damage that further transforms elongated tubules into large spheres (Fig. 10 B). Increased oxidative damage to mitochondrial proteins and/or lipids would lead to mitochondrial swelling. During swelling, long mitochondrial tubules seem to collapse and partially sever, presumably due to a Drp1-independent mechanism for division. Our data indicate that, depending on their ROS levels, mitochondria display elongated tubules, large spheres, or mixed morphology after loss of division.

In addition to morphological alterations, oxidative damage to mitochondrial proteins, lipids, and DNA could also lead

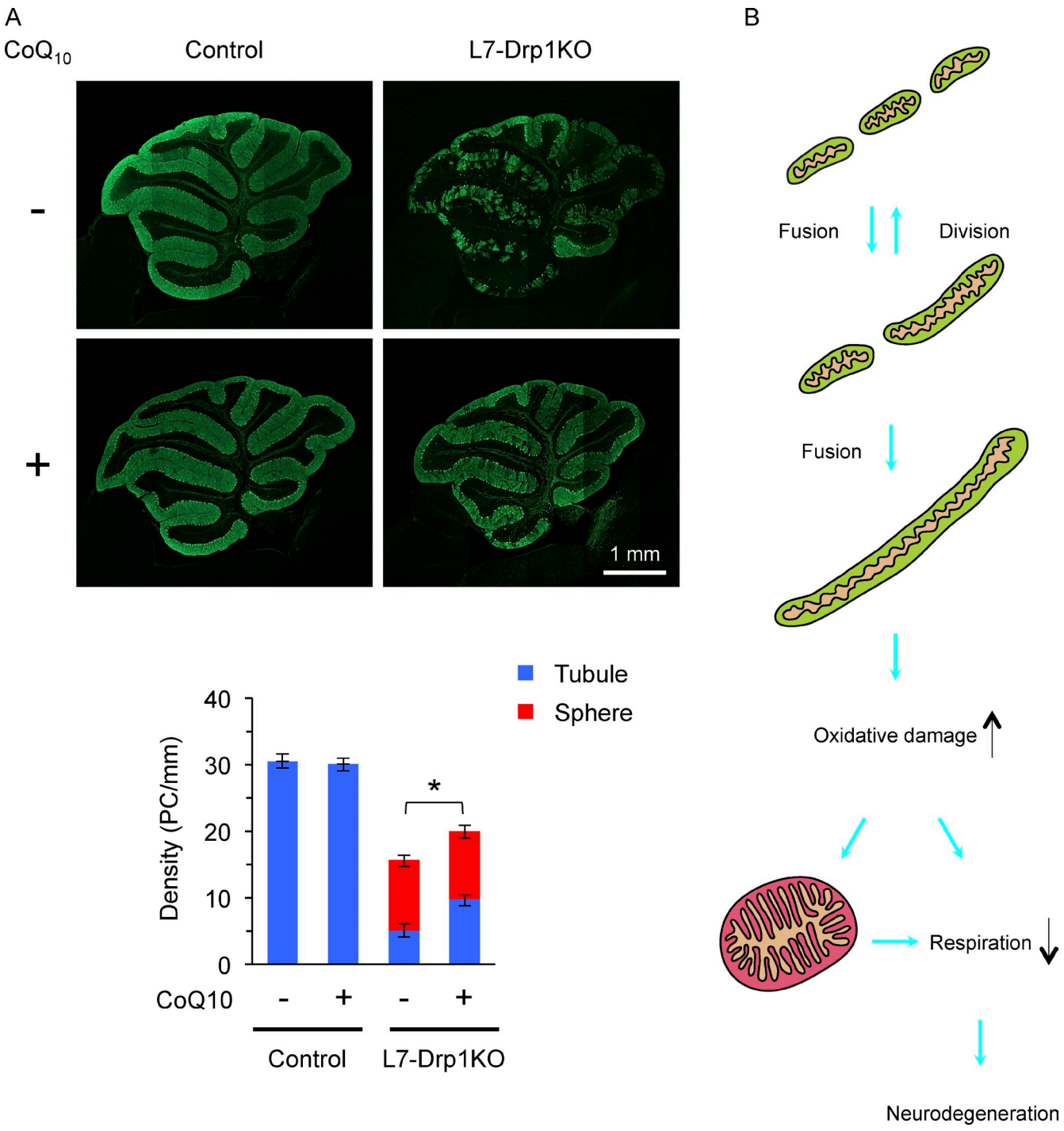


Figure 10. **Coenzyme Q10 suppresses Purkinje cell degeneration in L7-Drp1KO mice.** (A) Control and L7-Drp1KO mice were fed control and 1% coenzyme Q10–containing diets from 3 wk to 3 mo of age and then examined by immunofluorescence using antibodies specific to Car8 and PDH. Shown are cerebellar sagittal sections around the median line that were stained by the anti-Car8 antibodies. The number of soma of Purkinje cells (PC) that contained tubular (blue) and swollen (red) mitochondria was determined and normalized relative to the length of the Purkinje cell layer. Values represent the mean ± SEM ($n \geq 5$). (B) A model for neurodegeneration caused by mitochondrial division deficiency. In wild-type cells, mitochondria fuse and divide, as well as maintain a short tubular morphology. When mitochondrial division is blocked, the organelles elongate due to imbalanced, excess fusion. Elongated tubules accumulate oxidative damage, which leads to swelling of mitochondria and impairment of the electron transport chain. Mitochondrial enlargement may also decrease respiratory competence. Eventually, this decline in respiration causes neuronal death.

to a functional decline in Drp1KO Purkinje cells. We show that elongation of mitochondria by division deficiency itself does not promote neuronal cell death, but instead renders this organelle susceptible to ROS. These data suggest that the maintenance of respiratory competence requires mitochondrial division under increased ROS conditions. With antioxidant treatment, the requirement of mitochondrial division for neuronal survival was decreased. We did not directly measure electron transport

chain complex activity in antioxidant-treated Drp1KO Purkinje cells. However, because neurons are highly dependent on oxidative phosphorylation (Bolaños et al., 2010), it is reasonable to assume that this process is at least partially maintained at a level that is sufficient to support survival of Purkinje cells. In addition to oxidative damage, enlargement may affect mitochondrial functions by changing the volume-to-surface ratio of this organelle. Furthermore, reduced electron transport chain activities would generate more ROS and further affect mitochondrial shape and functions.

Our current study is consistent with previous studies showing that requirement of mitochondrial division in respiratory function varies among different cell culture systems. For instance, Drp1 knockdown in HeLa cells led to increased oxidative damage and decreased respiratory activities while Drp1KO MEFs maintain normal respiration and ATP levels (Benard et al., 2007; Parone et al., 2008; Ishihara et al., 2009; Wakabayashi et al., 2009). ROS levels or the susceptibility to ROS may be different in these cells.

A previous study has shown that efficient mitochondrial transport requires Drp1-dependent division to deliver these organelles into dendritic protrusions in response to synaptic stimulation (Li et al., 2004). When mitochondrial division is blocked, synapse formation is inhibited. In our current study, mitochondrial division is also critical to moving mitochondria into dendrites during neurite growth. These findings support the importance of mitochondrial size during movement through narrow cytoplasmic projections to their final destinations in polarized cells. Altered mitochondrial distribution likely affects the function and formation of synapses as well as the survival of neurons (Sheng and Cai, 2012).

The requirement of mitochondrial division in neuronal survival may explain why neurons are highly susceptible to defects in mitochondrial division in human disease. Neurons likely produce high levels of ROS and contain relatively fewer antioxidant molecules (Cui et al., 2004; Fatokun et al., 2008). Consistent with the vulnerability of Purkinje cells to mitochondrial division deficiency, these cells are one of the largest neurons and maintain exceptionally abundant connections with other neurons, thereby leading to a high metabolic demand and high levels of ROS (Kern and Jones, 2006). Also, it is important to consider that postmitotic neurons do not proliferate and therefore likely need to replace "old" mitochondria that may accumulate oxidative damage. In contrast, proliferating MEFs continuously generate new mitochondria; therefore, oxidative damage may be diluted and maintained at relatively low levels even without mitochondrial division. Mitochondrial turnover would be a critical quality control mechanism in neurons and plays a less important role in proliferating cells such as MEFs.

How does mitochondrial division contribute to mitochondrial quality control in Purkinje cells? Previous studies have shown that without mitochondrial division, mitochondria are not efficiently degraded by mitophagy, therefore resulting in an accumulation of oxidative damage (Wikstrom et al., 2009; Youle and Narendra, 2011). Supporting these studies, we observed that oxidative damage and ubiquitinated proteins associated with swollen mitochondria in Drp1KO Purkinje cells. These swollen mitochondria also accumulated mitophagy-related proteins such as LC3 and p62/SQSTM1. Because mitochondrial accumulation of these proteins suggests suppression and/or promotion of mitophagy (Klionsky et al., 2008), it would be interesting to test these possibilities in Drp1KO Purkinje cells in future studies. The E3 ubiquitin ligase parkin has been suggested to ubiquitinate mitochondrial proteins to promote mitophagy. In contrast, we found that parkin is dispensable for mitochondrial ubiquitination in Drp1KO Purkinje cells. Reports have shown that conditional ParkinKO mice, but not complete ParkinKO mice, exhibit neurodegenerative phenotypes (Von Coelln et al., 2004; Shin et al., 2011); thus, there may be additional E3 ubiquitin ligases that mediate mitochondrial quality control. In conclusion, our experiments provide evidence for a protective role for mitochondrial division against oxidative damage and neurodegeneration.

## Materials and methods

### Mice

All animal work was done according to guidelines established by the Johns Hopkins University Committee on Animal Care. *Drp1*$^{flox/flox}$ mice have been described previously (Wakabayashi et al., 2009). In brief, we generated mouse strains carrying a neomycin-resistant marker flanked by FRT and loxP sites inserted next to exons 3 and 5 of the *Drp1* gene. These mice were crossed to a transgenic strain that ubiquitously expresses Flp recombinase and confirmed FRT recombination by PCR. These strains were bred to a wild-type strain and isolated mice heterozygous for the conditional allele, but not Flp recombinase (*Drp1*$^{flox/flox}$ mice). L7-Cre mice (Barski et al., 2000) were obtained from The Jackson Laboratory. By breeding, we generated L7-Drp1KO mice (L7-Cre$^{+/-}$ *Drp1*$^{flox/flox}$) and littermate controls (L7-Cre$^{+/-}$::*Drp1*$^{+/flox}$ and *Drp1*$^{flox/flox}$). The littermate controls were phenotypically wild type. To generate double knockout for Drp1 and parkin, L7-Drp1KO mice were crossed to *Parkin*$^{-/-}$ mice (ParkinKO; Von Coelln et al., 2004). To examine the effect of coenzyme Q10, female control and L7-Drp1KO mice were fed with control (D12450B; Research Diets, Inc.) and coenzyme Q10–containing (D12450B plus 1% coenzyme Q10; Kaneka) diets from 3 wk to 3 mo of age.

### Immunofluorescence of cerebellar sections

For immunofluorescence of cerebellar Purkinje cells with antibodies to Car8, COX subunit I, succinate dehydrogenase iron-sulfur subunit, PDH, and Pex14, paraffin-embedded sections were used. Mice were fixed by perfusing ice-cold 4% paraformaldehyde in phosphate-buffered saline (PBS). The brain was dissected, further fixed in 4% paraformaldehyde in PBS overnight at 4°C, and then embedded in paraffin. Sections were cut, deparaffinized, washed in PBS, and incubated 0.1 M EDTA (pH 8.0) for 20 min and blocked in 5–10% donkey serum. Samples were incubated with antibodies to Car8 (Wakabayashi et al., 2009), PDH (Mitosciences), COX subunit I (Mitosciences), succinate dehydrogenase iron-sulfur subunit (Mitosciences), or Pex14 (Wakabayashi et al., 2009) followed by the appropriate secondary antibodies. Samples were viewed using a laser-scanning confocal microscope (LSM510-Meta; Carl Zeiss) equipped with 10x (0.4 NA) and 100x (1.3 NA) PlanApo objectives.

For immunofluorescence with antibodies to Drp1, Tom20, and ubiquitin, we used frozen sections. Mice were fixed by perfusing ice-cold 4% paraformaldehyde in PBS. The brain was dissected, further fixed in 4% paraformaldehyde in PBS for 2 h at 4°C, and frozen in the OCT compound (Tissue-Tek). Frozen sections were cut, washed in PBS, and blocked in 5–10% donkey serum. Sections were incubated with antibodies to Car8, Drp1 (BD), ubiquitin (Invitrogen), and Tom20 (Santa Cruz Biotechnology, Inc.) followed by the appropriate secondary antibodies.

For immunofluorescence with anti-LC3 antibodies, brains were dissected and quick-frozen in isopentane precooled with liquid nitrogen for 10 s. Samples were wrapped in aluminum foil and placed into liquid nitrogen for at least 30 min. Frozen sections were cut and mounted onto glass slides. Sections were fixed in 4% paraformaldehyde in PBS for 20 min at room temperature, washed with PBS, and treated with 0.1 M

EDTA (pH 8.0) for 20 min. Samples were incubated with antibodies to LC3 (Novus Biologicals), Car8, and PDH followed by the appropriate secondary antibodies.

**Histochemical measurements of electron transport chain complex activity**
The activity of NADH dehydrogenase and cytochrome *c* oxidase (COX) was measured as described previously (De Paepe et al., 2009). Brains were dissected and quick-frozen in isopentane precooled with liquid nitrogen for 10 s. Samples were wrapped in aluminum foil and placed into liquid nitrogen for at least 30 min. Frozen brains were sectioned (8-µm thickness) and mounted onto glass slides. To measure NADH dehydrogenase activity, sections were incubated with 0.625 mg/ml NADH and 1.25 mg/ml nitro blue tertrazolium in PBS at 37°C. The reaction was terminated by rinsing with distilled water. For COX, sections were incubated with 0.5 mg/ml diaminobenzidine tetrahydrochloride, 2 µg/ml catalase, and 1 mg/ml cytochrome *c* in 28 mM phosphate buffer, pH 7.4. Samples were dehydrated, mounted, and viewed using a microscope (model BX51; Olympus) equipped with a DP-70 color camera and 10x (0.3 NA) UIS2 objectives.

**Rotarod test**
Mice were tested for their ability to maintain balance on an accelerating rotating rod using the Rotamex (Columbus Instruments) at the Behavior Core at the Johns Hopkins University School of Medicine, as described previously (Gadad et al., 2010). The rotating rod accelerated from 4 to 40 rpm over 5 min. The time elapsed before falling was recorded. Three trials were performed and results were averaged for each mouse.

**Electron microscopy**
The cerebellum was fixed by perfusing 3% paraformaldehyde, 1.5% glutaraldehyde, 2.5% sucrose, and 100 mM cacodylate, pH 7.4, overnight. Brains were dissected and further fixed for 2 d. After washing, the samples were postfixed in 2.7% $OsO_4$ and 167 mM cacodylate, pH 7.4, for 1 h on ice. After washes in water, samples were incubated in 2% uranyl acetate for 30 min. After dehydration using 50, 70, 90, and 100% ethanol and 100% propylene oxide, samples were embedded in Epon resin (Ted Pella). Ultrathin sections were obtained using an ultramicrotome (Ultracut E; Reichert-Jung), stained with 2% uranyl acetate and lead citrate, and viewed on an electron microscope (model H-7100; Hitachi).

**MEFs**
MEFs were isolated from *Drp1*$^{-/-}$ and littermate wild-type E10.5 embryos (Wakabayashi et al., 2009) and immortalized spontaneously by serial passage (over 30 times). MEFs were cultured in DME supplemented with 10% FBS.

**Lentiviruses**
Lentiviruses were generated as described previously (Lois et al., 2002; Takamiya et al., 2008). In brief, pFUW expressing the Cre recombinase and GFP in tandem, GFP, Cre recombinase, and the myc epitope were cotransduced into HEK293T cells with two other constructs, pΔ8.9 and pVSVG, using Lipofectamine 2000 (Invitrogen). 3 d after transfection, the supernatant of transduced cells containing released viruses was collected by centrifugation at 110,000 *g* at 4°C for 2.5 h. The pellet was resuspended in OPTI-MEM (Invitrogen). The viruses were quick-frozen in liquid nitrogen and stored at −80°C.

**Cerebellar neuron culture**
Cerebellar neurons were cultured as described previously (Furuya et al., 1998; Tabata et al., 2000). Cerebella from P0 *Drp1*$^{flox/flox}$ mice were dissected and incubated with 2 mg/ml papain in HBSS for 30 min at 33°C. After three washings with HBSS, cerebella were dissociated by pipetting ten times each with a regular Pasteur pipette and a fire-polished Pasteur pipette in seeding medium (100 µM putrescine, 30 nM sodium selenite, 10 µg/ml gentamycin, in DME/F12) supplemented with 10% fetal bovine serum, 10 U/ml DNaseI, and 12 mM $MgSO_4$. Cells were collected by centrifugation at 1,200 rpm for 5 min at 4°C and resuspended in 200 µl of seeding medium supplemented with 10% fetal bovine serum per cerebellum. This 200-µl cell suspension was plated onto a 3.5-cm coverslip-bottomed dish (P35G-0-14-C; MatTek), which was coated with 1 mg/ml poly-L-lysine in 100 mM borax buffer, pH 8.5, at 37°C for 2 d. After the neurons were incubated at 37°C for 3 h, 2.3 ml of seeding medium supplemented with 200 µg/ml transferrin, 40 nM progesterone, 20 µg/ml insulin, 0.5 ng/ml triiodothyronine, 100 µg/ml bovine serum albumin, and 5% fetal bovine serum were added to the dish. Half of the culture medium was replaced with seeding medium supplemented with 200 µg/ml transferrin, 40 nM progesterone, 20 µg/ml insulin, 0.5 ng/ml triiodothyronine, 100 µg/ml BSA, and 4 µM cytosin arabinoside every 4 d. For lentiviral infection, viruses were added to the culture medium at d 0 or 7.

**Immunofluorescence of cultured cells**
For immunofluorescence of cultured MEFs and Purkinje cells, cells were fixed in prewarmed 4% paraformaldehyde in PBS for 20 min, washed with PBS three times, and permeabilized with 0.1% Triton X-100 in PBS for 10 min. After blocking in PBS containing 0.5% BSA and/or 10% donkey serum, cells were incubated overnight with antibodies to calbindin (Frontier Science), PDH, Tom20, ubiquitin, HNE (Abcam), LC3 (Novus Biologicals), and p62/SQSTM1 (Abcam), followed by the appropriate secondary antibodies. Cells were viewed using a laser-scanning confocal microscope (LSM510-Meta; Carl Zeiss). ImageJ (NIH, Bethesda, MD) and Adobe Photoshop software were used to analyze images. To quantify the number of Purkinje cells, non-overlapping 16 images, which covered an area of 64 $mm^2$, were obtained for each sample using a microscope (model IX81; Olympus) equipped with a camera (model C9100-02; Hamamatsu Photonics) and 4x (0.16 NA) and 10x (0.3 NA) UIS2 objectives.

**Statistics**
P-values were determined using the Student's *t* test: *, $P < 0.05$; **, $P < 0.01$; ***, $P < 0.001$.

**Online supplemental material**
Fig. S1 shows loss of Drp1 in Purkinje cells of L7-Drp1KO mice. Fig. S2 shows decreased levels of cytochrome *c* oxidase subunit I in L7-Drp1KO Purkinje cells. Fig. S3 shows the morphology of mitochondria in MEFs treated with *N*-acetylcysteine, carbonylcyanide-3-chlorophenylhydrazone, and nocodazole. Fig. S4 shows mitochondria distribution during neurite extension. Fig. S5 shows that mitoQ suppresses mitochondrial swelling in Drp1KO Purkinje cells. Online supplemental material is available at http://www.jcb.org/cgi/content/full/jcb.201110034/DC1.

We thank Yuanzheng Gao for assistance with Purkinje cell culture; Kogo Takamiya and Richard Huganir for lentiviral plasmids; Yasushi Tamura for preparing the model figure; and members of the Iijima and Sesaki laboratories for helpful discussion. We are grateful to Dr. Ted M. Dawson (Johns Hopkins University, Baltimore, MD) for kindly providing *Parkin*$^{-/-}$ mice and to Dr. Michael Murphy (Medical Research Council, UK) for MitoQ.

This work was supported by National Institutes of Health grants (AG028072 and RR000163 to P.H. Reddy, GM084015 to M. Iijima, and GM089853 to H. Sesaki).

Submitted: 7 October 2011
Accepted: 5 April 2012

## References

Alavi, M.V., S. Bette, S. Schimpf, F. Schuettauf, U. Schraermeyer, H.F. Wehrl, L. Ruttiger, S.C. Beck, F. Tonagel, B.J. Pichler, et al. 2007. A splice site mutation in the murine Opa1 gene features pathology of autosomal dominant optic atrophy. *Brain*. 130:1029–1042. http://dx.doi.org/10.1093/brain/awm005

Alexander, C., M. Votruba, U.E. Pesch, D.L. Thiselton, S. Mayer, A. Moore, M. Rodriguez, U. Kellner, B. Leo-Kottler, G. Auburger, et al. 2000. OPA1, encoding a dynamin-related GTPase, is mutated in autosomal dominant optic atrophy linked to chromosome 3q28. *Nat. Genet.* 26:211–215. http://dx.doi.org/10.1038/79944

Barski, J.J., K. Dethleffsen, and M. Meyer. 2000. Cre recombinase expression in cerebellar Purkinje cells. *Genesis*. 28:93–98. http://dx.doi.org/10.1002/1526-968X(200011/12)28:3/4<93::AID-GENE10>3.0.CO;2-W

Benard, G., N. Bellance, D. James, P. Parrone, H. Fernandez, T. Letellier, and R. Rossignol. 2007. Mitochondrial bioenergetics and structural network organization. *J. Cell Sci.* 120:838–848. http://dx.doi.org/10.1242/jcs.03381

Bolaños, J.P., A. Almeida, and S. Moncada. 2010. Glycolysis: a bioenergetic or a survival pathway? *Trends Biochem. Sci.* 35:145–149. http://dx.doi.org/10.1016/j.tibs.2009.10.006

Chang, C.R., and C. Blackstone. 2010. Dynamic regulation of mitochondrial fission through modification of the dynamin-related protein Drp1. *Ann. N. Y. Acad. Sci.* 1201:34–39. http://dx.doi.org/10.1111/j.1749-6632.2010.05629.x

Chen, H., S.A. Detmer, A.J. Ewald, E.E. Griffin, S.E. Fraser, and D.C. Chan. 2003. Mitofusins Mfn1 and Mfn2 coordinately regulate mitochondrial fusion and are essential for embryonic development. *J. Cell Biol.* 160:189–200. http://dx.doi.org/10.1083/jcb.200211046

Chen, H., J.M. McCaffery, and D.C. Chan. 2007. Mitochondrial fusion protects against neurodegeneration in the cerebellum. *Cell*. 130:548–562. http://dx.doi.org/10.1016/j.cell.2007.06.026

Chen, H., M. Vermulst, Y.E. Wang, A. Chomyn, T.A. Prolla, J.M. McCaffery, and D.C. Chan. 2010. Mitochondrial fusion is required for mtDNA stability in skeletal muscle and tolerance of mtDNA mutations. *Cell*. 141:280–289. http://dx.doi.org/10.1016/j.cell.2010.02.026

Cheung, E.C., H.M. McBride, and R.S. Slack. 2007. Mitochondrial dynamics in the regulation of neuronal cell death. *Apoptosis*. 12:979–992. http://dx.doi.org/10.1007/s10495-007-0745-5

Chizhikov, V., and K.J. Millen. 2003. Development and malformations of the cerebellum in mice. *Mol. Genet. Metab.* 80:54–65. http://dx.doi.org/10.1016/j.ymgme.2003.08.019

Cho, D.H., T. Nakamura, and S.A. Lipton. 2010. Mitochondrial dynamics in cell death and neurodegeneration. *Cell. Mol. Life Sci.* 67:3435–3447. http://dx.doi.org/10.1007/s00018-010-0435-2

Cui, K., X. Luo, K. Xu, and M.R. Ven Murthy. 2004. Role of oxidative stress in neurodegeneration: recent developments in assay methods for oxidative stress and nutraceutical antioxidants. *Prog. Neuropsychopharmacol. Biol. Psychiatry*. 28:771–799. http://dx.doi.org/10.1016/j.pnpbp.2004.05.023

Davies, V.J., A.J. Hollins, M.J. Piechota, W. Yip, J.R. Davies, K.E. White, P.P. Nicols, M.E. Boulton, and M. Votruba. 2007. Opa1 deficiency in a mouse model of autosomal dominant optic atrophy impairs mitochondrial morphology, optic nerve structure and visual function. *Hum. Mol. Genet.* 16:1307–1318. http://dx.doi.org/10.1093/hmg/ddm079

De Paepe, B., J.L. De Bleecker, and R. Van Coster. 2009. Histochemical methods for the diagnosis of mitochondrial diseases. *Curr. Protoc. Hum. Genet*. Chapter 19:Unit19 12.

Delettre, C., G. Lenaers, J.M. Griffoin, N. Gigarel, C. Lorenzo, P. Belenguer, L. Pelloquin, J. Grosgeorge, C. Turc-Carel, E. Perret, et al. 2000. Nuclear gene OPA1, encoding a mitochondrial dynamin-related protein, is mutated in dominant optic atrophy. *Nat. Genet.* 26:207–210. http://dx.doi.org/10.1038/79936

Fatokun, A.A., T.W. Stone, and R.A. Smith. 2008. Oxidative stress in neurodegeneration and available means of protection. *Front. Biosci.* 13:3288–3311. http://dx.doi.org/10.2741/2926

Furuya, S., A. Makino, and Y. Hirabayashi. 1998. An improved method for culturing cerebellar Purkinje cells with differentiated dendrites under a mixed monolayer setting. *Brain Res. Brain Res. Protoc.* 3:192–198. http://dx.doi.org/10.1016/S1385-299X(98)00040-3

Gadad, B.S., J.P. Daher, E.K. Hutchinson, C.F. Brayton, T.M. Dawson, M.V. Pletnikov, and J. Watson. 2010. Effect of fenbendazole on three behavioral tests in male C57BL/6N mice. *J. Am. Assoc. Lab. Anim. Sci.* 49:821–825.

Gandre-Babbe, S., and A.M. van der Bliek. 2008. The novel tail-anchored membrane protein Mff controls mitochondrial and peroxisomal fission in mammalian cells. *Mol. Biol. Cell*. 19:2402–2412. http://dx.doi.org/10.1091/mbc.E07-12-1287

Hatten, M.E., J. Alder, K. Zimmerman, and N. Heintz. 1997. Genes involved in cerebellar cell specification and differentiation. *Curr. Opin. Neurobiol.* 7:40–47. http://dx.doi.org/10.1016/S0959-4388(97)80118-3

Hoppins, S., and J. Nunnari. 2009. The molecular mechanism of mitochondrial fusion. *Biochim. Biophys. Acta*. 1793:20–26. http://dx.doi.org/10.1016/j.bbamcr.2008.07.005

Ishihara, N., M. Nomura, A. Jofuku, H. Kato, S.O. Suzuki, K. Masuda, H. Otera, Y. Nakanishi, I. Nonaka, Y. Goto, et al. 2009. Mitochondrial fission factor Drp1 is essential for embryonic development and synapse formation in mice. *Nat. Cell Biol.* 11:958–966. http://dx.doi.org/10.1038/ncb1907

James, D.I., P.A. Parone, Y. Mattenberger, and J.C. Martinou. 2003. hFis1, a novel component of the mammalian mitochondrial fission machinery. *J. Biol. Chem.* 278:36373–36379. http://dx.doi.org/10.1074/jbc.M303758200

Kageyama, Y., Z. Zhang, and H. Sesaki. 2011. Mitochondrial division: molecular machinery and physiological functions. *Curr. Opin. Cell Biol.* 23:427–434. http://dx.doi.org/10.1016/j.ceb.2011.04.009

Kern, J.K., and A.M. Jones. 2006. Evidence of toxicity, oxidative stress, and neuronal insult in autism. *J. Toxicol. Environ. Health B Crit. Rev.* 9:485–499. http://dx.doi.org/10.1080/10937400600882079

Klionsky, D.J., H. Abeliovich, P. Agostinis, D.K. Agrawal, G. Aliev, D.S. Askew, M. Baba, E.H. Baehrecke, B.A. Bahr, A. Ballabio, et al. 2008. Guidelines for the use and interpretation of assays for monitoring autophagy in higher eukaryotes. *Autophagy*. 4:151–175.

Lackner, L.L., J.S. Horner, and J. Nunnari. 2009. Mechanistic analysis of a dynamin effector. *Science*. 325:874–877. http://dx.doi.org/10.1126/science.1176921

Li, Z., K. Okamoto, Y. Hayashi, and M. Sheng. 2004. The importance of dendritic mitochondria in the morphogenesis and plasticity of spines and synapses. *Cell*. 119:873–887. http://dx.doi.org/10.1016/j.cell.2004.11.003

Lois, C., E.J. Hong, S. Pease, E.J. Brown, and D. Baltimore. 2002. Germline transmission and tissue-specific expression of transgenes delivered by lentiviral vectors. *Science*. 295:868–872. http://dx.doi.org/10.1126/science.1067081

Manczak, M., P. Mao, M.J. Calkins, A. Cornea, A.P. Reddy, M.P. Murphy, H.H. Szeto, B. Park, and P.H. Reddy. 2010. Mitochondria-targeted antioxidants protect against amyloid-beta toxicity in Alzheimer's disease neurons. *J. Alzheimers Dis.* 20(Suppl 2):S609–S631.

Muratani, M., and W.P. Tansey. 2003. How the ubiquitin-proteasome system controls transcription. *Nat. Rev. Mol. Cell Biol.* 4:192–201. http://dx.doi.org/10.1038/nrm1049

Narendra, D., A. Tanaka, D.F. Suen, and R.J. Youle. 2008. Parkin is recruited selectively to impaired mitochondria and promotes their autophagy. *J. Cell Biol.* 183:795–803. http://dx.doi.org/10.1083/jcb.200809125

Okamoto, K., and J.M. Shaw. 2005. Mitochondrial morphology and dynamics in yeast and multicellular eukaryotes. *Annu. Rev. Genet.* 39:503–536. http://dx.doi.org/10.1146/annurev.genet.38.072902.093019

Otera, H., C. Wang, M.M. Cleland, K. Setoguchi, S. Yokota, R.J. Youle, and K. Mihara. 2010. Mff is an essential factor for mitochondrial recruitment of Drp1 during mitochondrial fission in mammalian cells. *J. Cell Biol.* 191:1141–1158. http://dx.doi.org/10.1083/jcb.201007152

Palmer, C.S., L.D. Osellame, D. Laine, O.S. Koutsopoulos, A.E. Frazier, and M.T. Ryan. 2011. MiD49 and MiD51, new components of the mitochondrial fission machinery. *EMBO Rep.* 12:565–573. http://dx.doi.org/10.1038/embor.2011.54

Parone, P.A., S. Da Cruz, D. Tondera, Y. Mattenberger, D.I. James, P. Maechler, F. Barja, and J.C. Martinou. 2008. Preventing mitochondrial fission impairs mitochondrial function and leads to loss of mitochondrial DNA. *PLoS ONE*. 3:e3257. http://dx.doi.org/10.1371/journal.pone.0003257

Reddy, P.H., T.P. Reddy, M. Manczak, M.J. Calkins, U. Shirendeb, and P. Mao. 2011. Dynamin-related protein 1 and mitochondrial fragmentation in neurodegenerative diseases. *Brain Res. Brain Res. Rev.* 67:103–118. http://dx.doi.org/10.1016/j.brainresrev.2010.11.004

Schrader, M. 2006. Shared components of mitochondrial and peroxisomal division. *Biochim. Biophys. Acta*. 1763:531–541. http://dx.doi.org/10.1016/j.bbamcr.2006.01.004

Sheng, Z.H., and Q. Cai. 2012. Mitochondrial transport in neurons: impact on synaptic homeostasis and neurodegeneration. *Nat. Rev. Neurosci.* 13:77–93. http://dx.doi.org/10.1038/nrg3141

Shin, J.H., H.S. Ko, H. Kang, Y. Lee, Y.I. Lee, O. Pletinkova, J.C. Troconso, V.L. Dawson, and T.M. Dawson. 2011. PARIS (ZNF746) repression of PGC-1α contributes to neurodegeneration in Parkinson's disease. *Cell*. 144:689–702. http://dx.doi.org/10.1016/j.cell.2011.02.010

Smirnova, E., L. Griparic, D.L. Shurland, and A.M. van der Bliek. 2001. Dynamin-related protein Drp1 is required for mitochondrial division in mammalian cells. *Mol. Biol. Cell.* 12:2245–2256.

Tabata, T., S. Sawada, K. Araki, Y. Bono, S. Furuya, and M. Kano. 2000. A reliable method for culture of dissociated mouse cerebellar cells enriched for Purkinje neurons. *J. Neurosci. Methods*. 104:45–53. http://dx.doi.org/10.1016/S0165-0270(00)00323-X

Takamiya, K., L. Mao, R.L. Huganir, and D.J. Linden. 2008. The glutamate receptor-interacting protein family of GluR2-binding proteins is required for long-term synaptic depression expression in cerebellar Purkinje cells. *J. Neurosci.* 28:5752–5755. http://dx.doi.org/10.1523/JNEUROSCI.0654-08.2008

Tamura, Y., K. Itoh, and H. Sesaki. 2011. SnapShot: Mitochondrial dynamics. *Cell*. 145:1158, 1158.e1. http://dx.doi.org/10.1016/j.cell.2011.06.018

Tanaka, A., M.M. Cleland, S. Xu, D.P. Narendra, D.F. Suen, M. Karbowski, and R.J. Youle. 2010. Proteasome and p97 mediate mitophagy and degradation of mitofusins induced by Parkin. *J. Cell Biol.* 191:1367–1380. http://dx.doi.org/10.1083/jcb.201007013

Twig, G., A. Elorza, A.J. Molina, H. Mohamed, J.D. Wikstrom, G. Walzer, L. Stiles, S.E. Haigh, S. Katz, G. Las, et al. 2008. Fission and selective fusion govern mitochondrial segregation and elimination by autophagy. *EMBO J.* 27:433–446. http://dx.doi.org/10.1038/sj.emboj.7601963

Von Coelln, R., B. Thomas, J.M. Savitt, K.L. Lim, M. Sasaki, E.J. Hess, V.L. Dawson, and T.M. Dawson. 2004. Loss of locus coeruleus neurons and reduced startle in parkin null mice. *Proc. Natl. Acad. Sci. USA*. 101:10744–10749. http://dx.doi.org/10.1073/pnas.0401297101

Wakabayashi, J., Z. Zhang, N. Wakabayashi, Y. Tamura, M. Fukaya, T.W. Kensler, M. Iijima, and H. Sesaki. 2009. The dynamin-related GTPase Drp1 is required for embryonic and brain development in mice. *J. Cell Biol.* 186:805–816. http://dx.doi.org/10.1083/jcb.200903065

Waterham, H.R., J. Koster, C.W. van Roermund, P.A. Mooyer, R.J. Wanders, and J.V. Leonard. 2007. A lethal defect of mitochondrial and peroxisomal fission. *N. Engl. J. Med.* 356:1736–1741. http://dx.doi.org/10.1056/NEJMoa064436

Westermann, B. 2010. Mitochondrial fusion and fission in cell life and death. *Nat. Rev. Mol. Cell Biol.* 11:872–884. http://dx.doi.org/10.1038/nrm3013

Wikstrom, J.D., G. Twig, and O.S. Shirihai. 2009. What can mitochondrial heterogeneity tell us about mitochondrial dynamics and autophagy? *Int. J. Biochem. Cell Biol.* 41:1914–1927. http://dx.doi.org/10.1016/j.biocel.2009.06.006

Yoon, Y., K.R. Pitts, and M.A. McNiven. 2001. Mammalian dynamin-like protein DLP1 tubulates membranes. *Mol. Biol. Cell*. 12:2894–2905.

Yoon, Y., E.W. Krueger, B.J. Oswald, and M.A. McNiven. 2003. The mitochondrial protein hFis1 regulates mitochondrial fission in mammalian cells through an interaction with the dynamin-like protein DLP1. *Mol. Cell. Biol.* 23:5409–5420. http://dx.doi.org/10.1128/MCB.23.15.5409-5420.2003

Yoshii, S.R., C. Kishi, N. Ishihara, and N. Mizushima. 2011. Parkin mediates proteasome-dependent protein degradation and rupture of the outer mitochondrial membrane. *J. Biol. Chem.* 286:19630–19640. http://dx.doi.org/10.1074/jbc.M110.209338

Youle, R.J., and D.P. Narendra. 2011. Mechanisms of mitophagy. *Nat. Rev. Mol. Cell Biol.* 12:9–14. http://dx.doi.org/10.1038/nrm3028

Zhang, Z., N. Wakabayashi, J. Wakabayashi, Y. Tamura, W.J. Song, S. Sereda, P. Clerc, B.M. Polster, S.M. Aja, M.V. Pletnikov, et al. 2011. The dynamin-related GTPase Opa1 is required for glucose-stimulated ATP production in pancreatic beta cells. *Mol. Biol. Cell*. 22:2235–2245. http://dx.doi.org/10.1091/mbc.E10-12-0933

Züchner, S., I.V. Mersiyanova, M. Muglia, N. Bissar-Tadmouri, J. Rochelle, E.L. Dadali, M. Zappia, E. Nelis, A. Patitucci, J. Senderek, et al. 2004. Mutations in the mitochondrial GTPase mitofusin 2 cause Charcot-Marie-Tooth neuropathy type 2A. *Nat. Genet.* 36:449–451. http://dx.doi.org/10.1038/ng1341